

# Connexin-43 in the osteogenic BM niche regulates its cellular composition and the bidirectional traffic of hematopoietic stem cells and progenitors

Daniel Gonzalez-Nieto,<sup>1,2</sup> Lina Li,<sup>3</sup> Anja Kohler,<sup>4</sup> Gabriel Ghiaur,<sup>1</sup> Eri Ishikawa,<sup>3</sup> Amitava Sengupta,<sup>1</sup> Malav Madhu,<sup>1</sup> Jordan L. Arnett,<sup>1</sup> Rebecca A. Santho,<sup>1</sup> Susan K. Dunn,<sup>3</sup> Glenn I. Fishman,<sup>5</sup> David E. Gutstein,<sup>5,6</sup> Roberto Civitelli,<sup>7</sup> Luis C. Barrio,<sup>8</sup> Matthias Gunzer,<sup>4</sup> and Jose A. Cancelas<sup>1,3</sup>

<sup>1</sup>Division of Experimental Hematology and Cancer Biology, Cincinnati Children's Hospital Medical Center, Cincinnati, OH; <sup>2</sup>Bioengineering and Telemedicine Group, Center for Biomedical Technology, Universidad Politécnica de Madrid, Spain; <sup>3</sup>Hoxworth Blood Center, University of Cincinnati, Cincinnati, OH; <sup>4</sup>Institute of Molecular and Clinical Immunology, Otto von Guericke University, Magdeburg, Germany; <sup>5</sup>Leon H. Charney Division of Cardiology, New York University, Langone Medical Center, New York, NY; <sup>6</sup>Merck Sharp and Dohme Corp, Rahway, NJ; <sup>7</sup>Division of Bone and Mineral Diseases, Department of Internal Medicine, Washington University, St Louis, MO; and <sup>8</sup>Unit of Experimental Neurology, Hospital Ramon y Cajal, Madrid, Spain

**Connexin-43 (Cx43), a gap junction protein involved in control of cell proliferation, differentiation and migration, has been suggested to have a role in hematopoiesis. Cx43 is highly expressed in osteoblasts and osteogenic progenitors (OB/P). To elucidate the biologic function of Cx43 in the hematopoietic microenvironment (HM) and its influence in hematopoietic stem cell (HSC) activity, we studied the hematopoietic function in an**

**in vivo model of constitutive deficiency of Cx43 in OB/P. The deficiency of Cx43 in OB/P cells does not impair the steady state hematopoiesis, but disrupts the directional trafficking of HSC/progenitors (Ps) between the bone marrow (BM) and peripheral blood (PB). OB/P Cx43 is a crucial positive regulator of transstromal migration and homing of both HSCs and progenitors in an irradiated microenvironment. However, OB/P Cx43 deficiency in**

**nonmyeloablated animals does not result in a homing defect but induces increased endosteal lodging and decreased mobilization of HSC/Ps associated with proliferation and expansion of Cxcl12-secreting mesenchymal/osteolineage cells in the BM HM in vivo. Cx43 controls the cellular content of the BM osteogenic microenvironment and is required for homing of HSC/Ps in myeloablated animals. (*Blood*. 2012;119(22):5144-5154)**

## Introduction

In the adult bone marrow (BM), the hematopoietic function is supported by the proliferation and differentiation of a finite number of transplantable hematopoietic stem cells and progenitors (HSCs/Ps) that have self-renewal and multipotential differentiation capacity. Endosteal and neighboring vascular/perivascular niches have been proposed as anatomic sites that control HSC/P activity, providing signals that regulate the stem cell pool size, survival, and migration.<sup>1-4</sup> The definition of the cell components of the BM hematopoietic microenvironment (HM) is an area of debate. Endothelial cells,<sup>2</sup> mesenchymal stem cells (MSCs),<sup>5</sup> and osteoblasts and osteogenic progenitors (OB/Ps)<sup>1,4,6</sup> represent major cell components of the BM HM.

A poorly studied mechanism of intercellular communication (IC) in the HM is mediated by gap junction (GJ) channels. GJ channels are formed by a large family of proteins called connexins (Cxs). Each neighboring cell contributes cell-to-cell channels with 1 hemichannel that dock head-to-head. GJ channels have the ability to transfer ions and low-molecular weight secondary messengers from one cell to another depending on concentration gradients and Cx-dependent selective permeability.<sup>7</sup> Connexin-43 (Cx43), one member of this protein family, is highly expressed by adult BM stromal cells,<sup>8</sup> osteoblasts,<sup>9</sup> endothelial cells,<sup>2</sup> and MSCs,<sup>5</sup> and is also expressed by HSCs.<sup>10</sup> The presence of a functional Cx43-dependence of GJIC between osteoblasts and stromal cells, as well as between stromal cells and HSCs, has been confirmed in vitro.<sup>11</sup>

After HSC transplantation, HSCs must first home to the BM, and then localize and anchor in suitable microenvironments within the BM, a process known as lodgment.<sup>12</sup> This process involves the migration of HSC/Ps through different layers of cell components in the HM, including endothelial cells and mesenchymal-origin cells, which act as extrinsic HSC/P migration regulators,<sup>13</sup> and is directed by chemokine gradients. Myeloablation through irradiation has been postulated to modify the functional ability of the BM HM to allow HSC homing and retention through clearance of HSC niches.<sup>14</sup> The effect of irradiation on the BM HM is not well known, but diverse studies have shown that it is not innocuous<sup>15</sup> and includes the up-regulation of expression and secretion of Cxcl12<sup>16</sup> and the up-regulation of the expression of Cx43 in the BM.<sup>17</sup> It has been proposed that Cx43 hemichannels are important in reinforcing cell-to-cell migration and that Cx43-dependent GJ are needed in the process of neuronal migration during neocortex formation.<sup>18,19</sup> Whether Cx43 expression controls the processes of migration of HSC/Ps within the HM is unknown.

Here, we analyzed the specific role played by Cx43 in the OB/P HM using conditionally osteoblast-lineage specific Cx43-deficient mice. Our results indicate that OB/P Cx43 expression is critical in maintaining the cell composition of the BM osteogenic microenvironment, in controlling the content of Cxcl12-expressing cells in the HSC niche, and in the lodging and mobilization of HSC/Ps in nonmyeloablated animals. In contrast, Cx43-deficiency in an

Submitted July 19, 2011; accepted March 18, 2012. Prepublished online as Blood First Edition paper, April 12, 2012; DOI 10.1182/blood-2011-07-368506.

The publication costs of this article were defrayed in part by page charge payment. Therefore, and solely to indicate this fact, this article is hereby marked "advertisement" in accordance with 18 USC section 1734.

The online version of this article contains a data supplement.

© 2012 by The American Society of Hematology

irradiated HM, results in the impairment of homing, transstromal migration, radioprotection, and engraftment of BM HSCs.

## Methods

### Animals

Osteolineage (*OB/P*)–*Cx43*–deficient mice were generated using genetically modified (2.3 Kb) *Colα1(I)–Cre–Cx43<sup>fllox/fllox</sup>* mice.<sup>20</sup> *Colα1(I)–Cre* mice were crossed with *Rosa-loxP–STOP–loxP–lacZ* reporter mice for microanatomical analysis of β-galactosidase positive cells as previously described.<sup>21</sup> *Hematopoietic–Cx43 (H–Cx43)*–deficient mice were generated using *Vav1–Cre–Cx43<sup>fllox/fllox</sup>* mice.<sup>22</sup> In some experiments, we used *Mx1–Cre–Cx43<sup>fllox/fllox</sup>* mice, in which inactivation of *Cx43* in the whole BM was induced by intraperitoneal administration of double-stranded RNA polyinosinic-polycytidylic acid (polyI:C; Amersham Pharmacia Biotech) that promoted interferon production leading to the activation of *Mx1* promoter.<sup>22</sup> *Colα1(I)–Cre*; wild-type (WT), *Vav1–Cre*;WT or polyI:C-treated *Mx1–Cre*;WT mice served as controls. Animals were backcrossed for a minimum of 5 generations into C57Bl/6 background. Ubiquitin C-enhanced green fluorescence protein (EGFP) mice were described elsewhere.<sup>23</sup> Animals were bred and housed in the AALAC-accredited animal facility of Cincinnati Children's Hospital Medical Center, or purchased from The Jackson Laboratory. All the experiments were carried out under animal protocols approved by the Cincinnati Children's Hospital Institutional Animal Committee in conformance with all relevant regulatory standards for animal care.

### Analysis of BM cell subpopulations by flow cytometry

The BM content of HSC/Ps was immunophenotypically assessed as previously described.<sup>22</sup> The frequency of nonhematopoietic cells containing osteolineage cells and other mesenchymal cells was quantified by flow cytometry analysis of *CD45<sup>+</sup>/Ter119<sup>–</sup>* (APC-*CD45* and APC-*Ter119*; e-Bioscience) BM cells. For further quantification of osteolineage cell populations, goat anti-mouse cadherin-11 (Santa Cruz Biotechnology) and rabbit anti-mouse *Cxcl12* (Abcam) antibodies were used, followed by incubation with donkey anti-goat-PE and donkey anti-rabbit-PerCP-Cy5.5 (Santa Cruz Biotechnology). After incubation with primary and secondary antibodies (anti-*CD45*, anti-*Ter119*, anti-cadherin-11, and donkey anti-goat-PE), cells were fixed, permeabilized (Cytfix/Cytoperm; BD Bioscience), stained with a rabbit anti-mouse *Cxcl12* antibody, and subsequent labeled with donkey anti-rabbit-PerCP-Cy5.5 antibody as described.<sup>24</sup> All analysis tubes were processed for fixation/permeabilization. Using cadherin-11 as a highly expressed marker of osteolineage cells, including osteoprogenitors and *nestin<sup>+</sup>*, hematopoiesis-supporting MSCs,<sup>5,25</sup> we defined the osteolineage population as *CD45<sup>+</sup>*, *Ter119<sup>–</sup>*, and *cadherin-11<sup>+</sup>*, whereas the remaining mesenchymal cells were defined as *CD45<sup>+</sup>*, *Ter119<sup>–</sup>*, and *cadherin-11<sup>–</sup>*. Gating consisted of a first gate applied to cells stained with an isotype control (to identify the *CD45<sup>+</sup>/Ter119<sup>–</sup>* cell population); a second gate applied to *CD45<sup>+</sup>/Ter119<sup>–</sup>* cells to analyze cadherin-11 expressing populations, based on a preimmune goat serum staining set; and a third gate applied to *CD45<sup>+</sup>/Ter119<sup>–</sup>/cadherin<sup>+</sup>* or *CD45<sup>+</sup>/Ter119<sup>–</sup>/cadherin<sup>–</sup>* BM cells to define *Cxcl12* expression based on a control using preimmune rabbit serum.

### Homing assays

In myeloablated animals for hematopoietic progenitor homing<sup>26</sup>:  $20 \times 10^6$  BM donor cells were injected through the tail vein into lethally irradiated mice (700 + 475 cGy), split doses at a dose rate of 58 to 63 cGy/min; separated 3 hours, and previously demonstrated to eliminate all endogenous BM colony-forming units (CFU-C)<sup>27</sup> in control or *OB/P–Cx43*–deficient recipient mice. Sixteen hours after transplant, the recipient mice were killed and the BM cells of the lower limbs and pelvis were harvested and cultured in triplicate for CFU-C assay. To estimate the BM recovery, we considered that femora, tibiae, and pelvis contained 25% of the overall BM.<sup>28</sup> For *Lin<sup>–</sup>/c-kit<sup>+</sup>/Sca-1<sup>+</sup>* (LSK) cell homing, 85 000 to 100 000 sorted BM LSK cells stained with carboxyfluorescein

succinimidyl ester (CFSE) were transplanted and analyzed.<sup>27</sup> BM content of CFSE<sup>+</sup> cells was quantified by flow cytometry. For HSC homing,<sup>26</sup>  $20 \times 10^6$  BM WT *CD45.1<sup>+</sup>* cells were injected intravenously into lethally irradiated *CD45.2<sup>+</sup>* WT or *OB/P–Cx43*–deficient primary mice. Three hours later, the mice were killed and the BM cells were harvested and injected together with  $0.5 \times 10^6$  WT *CD45.2<sup>+</sup>* competitor BM cells into secondary lethally irradiated WT *CD45.2<sup>+</sup>* recipient mice. The homing percentage was calculated as the ratio between the output competitive repopulating units (CRUs) from mice transplanted with HSCs homed in WT or *OB/P–Cx43*–deficient mice, and input CRUs.

In nonmyeloablated animals, homing analysis was performed by transplanting intravenously  $1.9$  to  $3.5 \times 10^7$  BM cells from ubiquitin C-EGFP mice into nonmyeloablated animals and analyzing the femoral and PB content of EGFP<sup>+</sup>/*Lin<sup>–</sup>/c-kit<sup>+</sup>* and EGFP<sup>+</sup>/*Lin<sup>–</sup>/c-kit<sup>+</sup>/Sca-1<sup>+</sup>* cells 16 hours after transplantation. This same procedure was also used to analyze the fraction of circulating HSC/Ps in myeloablated animals. Intravital microscopy (IVM) of HSC/P distribution in the BM of nonmyeloablated animals was analyzed using time-lapse multiphoton IVM (MP-IVM, LSM 710 NLO microscope; Zeiss) of transplanted CFSE<sup>+</sup>/*Lin<sup>–</sup>/c-kit<sup>+</sup>* BM cells followed by infusion of rhodamine-dextran 16 hours later, with detection by an array of independent photomultiplier tube-detectors (nondescanned detectors; NDDs) was used to monitor cells in the tibiae of transplanted mice. The distance from the HSC/P to the endosteal surface immediately underneath the endosteal osteoblasts and their relationship with the endosteal vasculature was analyzed.<sup>29</sup> For imaging, a  $300 \times 300 \mu\text{m}$  area was scanned in 30 steps of  $4 \mu\text{m}$  each to a depth of  $120 \mu\text{m}$  (approximately 12 cell layers) using an illumination wavelength of 800 nm and the detection of green (530 nm) fluorescence as well as second-harmonic generation (SHG) signal (at 480 nm emission). The 3-D images were used to measure the distance of individual cells to the endosteal lining.<sup>29</sup>

### Engraftment assays

Radioprotection experiments were performed by transplanting a limiting dose ( $1 \times 10^4$ ) of congenic *CD45.1<sup>+</sup>* WT BM cells into control or *OB/P–Cx43*–deficient irradiated recipients. Mortality associated with hematopoiesis failure was determined at day 30 after transplantation. For long-term engraftment experiments,  $3 \times 10^5$  or  $1 \times 10^6$  WT *CD45.1<sup>+</sup>* BM cells were administered. The frequency of *CD45.1<sup>+</sup>* cells in PB was followed for up to 14 months. For secondary transplantation experiments,  $5 \times 10^6$  BM cells were transplanted into lethally irradiated C57Bl/6 recipients. To determine the content of PB HSCs, 400  $\mu\text{L}$  of PB from *CD45.2<sup>+</sup>* WT or *OB/P–Cx43*–deficient mice were mixed with  $5 \times 10^5$  WT *CD45.1<sup>+</sup>* cells as competitors and transplanted into lethally irradiated *CD45.1<sup>+</sup>* WT recipient mice.

### Stromal cell isolation, ex vivo expansion, and CFU-F/CFU-OB assays

BM cells were plated at a density of  $6.5 \times 10^5$  cells/cm<sup>2</sup> on fibronectin-coated wells (Corning) in Iscove modified Dulbecco medium (IMDM) supplemented with 20% of MSC stimulatory supplements (StemCell Technologies), 100  $\mu\text{M}$  2-mercaptoethanol, 100 IU/mL penicillin, 0.1 mg/mL streptomycin, 2mM L-glutamine, 10 ng/mL human platelet-derived growth factor (PDGF)–BB, and 10 ng/mL recombinant mouse epidermal growth factor (rM-EGF). Adherent clusters were grown for a minimum of 5 passages. Macrophage depletion was assessed by flow cytometry. All experiments were performed on stromal cells in passages 10 through 14. For CFU-fibroblast (F), BM cells were plated in the medium previously mentioned plus 40% of Methocult (StemCell Technologies). For CFU-OB, the same medium was supplemented with 0.1  $\mu\text{M}$  dexamethasone, 0.25mM ascorbic acid, and 10mM 2-glycerolphosphate (all Sigma-Aldrich) to induce osteoblastic differentiation. All cultures were incubated at 37°C, 5% CO<sub>2</sub>, and 100% humidity for 14 days. Adherent cell clusters containing > 50 cells were counted as a colonies. Osteoblast colonies were detected by alkaline phosphatase activity analysis (Sigma-Aldrich).

### Cxcl12 expression and secretion analysis

BM *Cxcl12* levels were determined in femora crunched in PBS containing a protease inhibitor cocktail (Roche Diagnostics). The cell suspension was

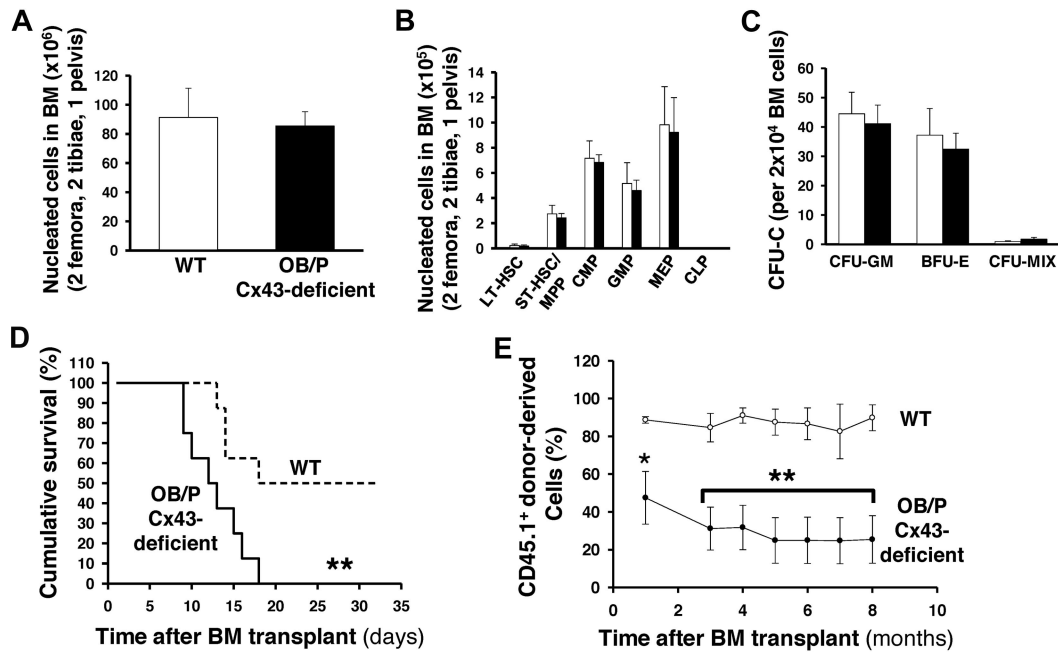


**Figure 1. Cx43 deficiency in OB/P compartments does not modify steady-state hematopoiesis but impair radioprotection in primary recipient mice.** (A) BM cellularity (2 femora, 2 tibiae, and pelvis) in WT and OB/P Cx43-deficient mice. (B) BM content of HSC/P subpopulations in WT and OB/P Cx43-deficient BM. LT indicates long-term; ST, short-term; MPP, multipotent progenitor; CMP, common myeloid progenitor; GMP, granulocyte/macrophage progenitors; MEP, megakaryocyte/erythroid progenitor; and CLP, common lymphoid progenitors. (C) Hematopoietic progenitor content (CFU-granulocyte-macrophage [GM], erythroid burst-forming units [BFU-E], and CFU-Mix) in the BM of WT and OB/P Cx43-deficient mice. (D) Survival curve of lethally irradiated WT (dashed line) or OB/P Cx43-deficient (solid line) recipient mice transplanted with  $1 \times 10^4$  WT BM cells (low dose). (E) Percentage of chimerism in WT (empty circles) and OB/P Cx43 deficient mice (solid circles) transplanted with  $3 \times 10^5$  WT CD45.1<sup>+</sup> BM cells. Data are shown as mean  $\pm$  SEM, of 2 independent experiments, with a minimum of 7 mice per group.

spun down. The cell pellet and supernatant were processed for lysate (Western blot) and extracellular Cxcl12 analysis (ELISA; R&D Systems), respectively. In explanted BM stromal cells, Cxcl12 expression analysis was performed similarly from stromal cell cultures. Values were normalized with respect to the total number of cells in every group and dish.

### HSC/P transstromal migration and stromal adhesion

Migration of hematopoietic progenitors through different types of mesenchymal stromal cells was performed by incubation of  $5 \times 10^4$  low density (LD) BM (LDBM) cells derived from control or hematopoietic-Cx43-deficient animals, on the top chamber of a 24-well transwell plate (Corning) containing a monolayer of irradiated (20 Gy) or not irradiated, freshly confluent WT or Cx43-deficient stromal cell lines. Recombinant Cxcl12 (100 ng/mL; R&D Systems) was placed in the bottom wells, and the 24-well plate was incubated at 37°C, 5% CO<sub>2</sub>. After 16 hours of incubation, cells from the bottom chamber were collected by trypsinization, washed in PBS, and the number of migrated hematopoietic progenitors was determined by CFU-C assay. Adhesion of HSC/Ps to mesenchymal stromal cells was performed by incubation of  $5 \times 10^4$  LDBM cells from control or Cx43-deficient (derived from H-Cx43-deficient mice) mice on the top of irradiated (20 Gy) freshly confluent stromal cells from control or Cx43-deficient (derived from OB/P-Cx43 deficient mice) mice previously cultured on 24 well-plates in stromal medium. After 1 to 3 hours, nonadherent cells were removed and incubated for CFU-C assay. All assays were performed in triplicate.

Other methods can be found in supplemental Methods (available on the *Blood* Web site; see the Supplemental Materials link at the top of the online article).

## Results

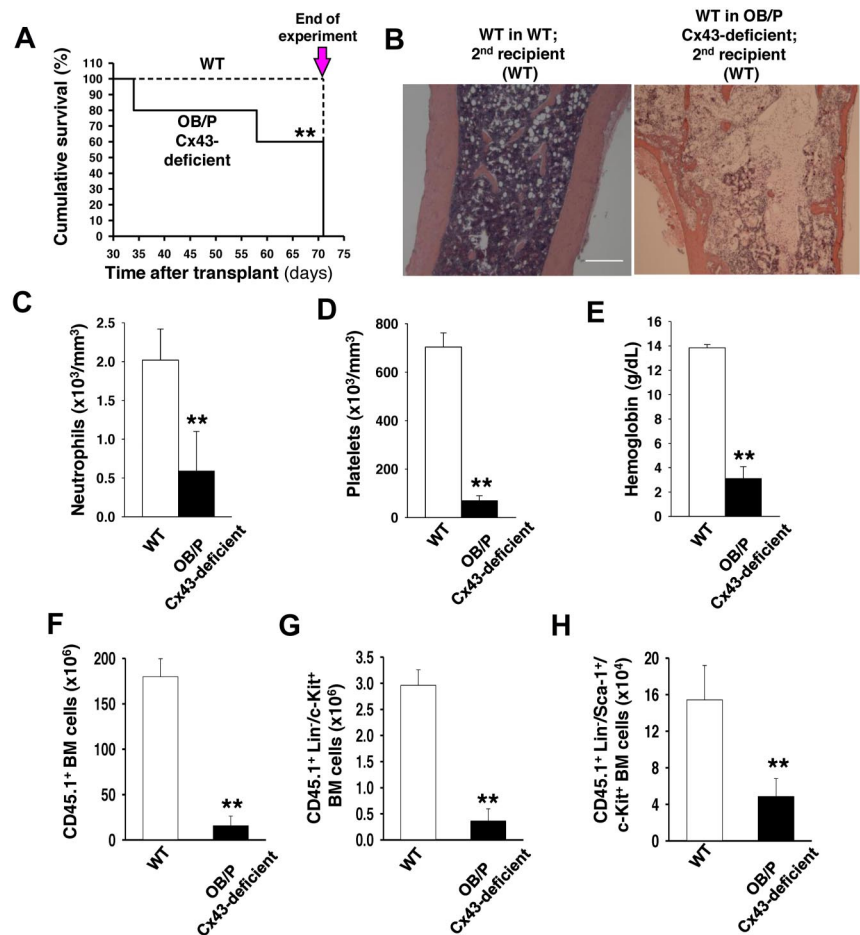
### Cx43 deficiency in OB/P Cx43-deficient mice does not impair steady-state hematopoiesis

We previously demonstrated that Cx43-deficiency in fetal liver stromal cells induced hematopoietic failure, using in vitro cobblestone-area-

forming cell (CAFC) assays.<sup>8</sup> Here, we analyzed whether Cx43 was required in osteogenic lineage cells, major cellular constituents of the BM stroma, to support hematopoiesis in vivo. We evaluated the effect of constitutive loss-of-function of Cx43 in these cells, using collagen type 1,  $\alpha 1$  (Col1- $\alpha 1$ )-Cx43<sup>flx/flx</sup> mice, which had been shown to induce osteoblast functional deficiency.<sup>20</sup> Cre recombinase expression driven by the Col1 $\alpha$ 1 promoter induced gene excision in osteocytes (located in the cortical bone) and in cells on or near the endosteal surface but not in multilineage hematopoiesis within the BM cavity (supplemental Figure 1A). Using cadherin-11, a highly expressed marker of osteolineage cells, including osteoprogenitors and nestin<sup>+</sup>, hematopoiesis-supporting MSCs,<sup>5,25</sup> we found that the expression of Cx43 was  $\sim 4$ -log diminished in BM OB/P cells, phenotypically defined as CD45<sup>-</sup>/Ter119<sup>-</sup>/cadherin-11<sup>+</sup>, derived from Col1- $\alpha 1$ -Cre;Cx43<sup>flx/flx</sup> mice compared with control but not in other HM cell constituents (CD45<sup>-</sup>/Ter119<sup>-</sup>/cadherin-11<sup>-</sup>, supplemental Figure 1B). Cx43 immunoblots revealed a drastic reduction in Cx43 protein expression in BM CFU-F from Col1- $\alpha 1$ -Cre;Cx43<sup>flx/flx</sup> mice (supplemental Figure 1C) because of Cx43 gene deletion (supplemental Figure 1D). Cx43 RNA and protein expression were also abolished in explanted macrophage-depleted stromal cells from the BM of Col1- $\alpha 1$ -Cre;Cx43<sup>flx/flx</sup> mice (supplemental Figure 1E-F). Thus, Col1- $\alpha 1$ -Cre;Cx43<sup>flx/flx</sup> mice have a severe deficiency of Cx43 in the BM OB/Ps and explanted stromal cells, well-recognized cell constituents of the HM.

The Col1- $\alpha 1$ -Cre;Cx43<sup>flx/flx</sup> (OB/P Cx43 deficient) mice demonstrate normal hematopoiesis in young mice (8 to 20 weeks old). The BM content of hematopoietic progenitors and immunophenotypically identified HSCs of OB/P Cx43-deficient is similar to BM from WT mice (Figure 1A-C), suggesting that the loss of function of Cx43 in BM osteogenic cells does not change steady state hematopoiesis or the content of phenotypically identified HSC/Ps in primary mice.

**Figure 2. OB/P Cx43 expression is required for progenitor-dependent radioprotection and serial transplantation engraftment of WT HSCs.** (A) Survival curve of secondary recipients of WT hematopoiesis from WT (dashed line) or OB/P Cx43-deficient primary recipients (solid line), which had been transplanted with  $1 \times 10^6$  WT BM cells (high dose). BM from primary recipient mice were pooled and transplanted into secondary recipients and analyzed. The remaining secondary recipient mice were killed on day 71 after transplantation and the experiment was terminated (arrow). (B) Representative micrographs (original magnification  $\times 10$ ; bar = 0.25 mm) of longitudinal femoral sections (H&E staining) of WT in WT secondary recipients and WT in OB/P Cx43-deficient secondary recipients. Micrographs were obtained with an Olympus CKX41, objectives  $\times 10$ ,  $\times 40$ , and  $\times 100$ . The images were acquired with a motican 2500 color camera (5.0 MPixel, USB2.0), Motich China Group Co Ltd, and processed using Motic Images Plus 2.0 software. (C-E) PB counts of control and WT hematopoiesis in OB/P Cx43-deficient secondary recipients on day 71 after transplantation. Empty bars represent data from WT controls; solid bars represent data from secondary recipients of WT hematopoiesis into OB/P Cx43-deficient hematopoiesis in primary recipients. (F-H) Quantification of BM cell populations from secondary recipients receiving WT chimeric BM from a primary recipient HM that was either WT (empty bar) or OB/P Cx43-deficient HM (solid bar). (F) Total CD45.1<sup>+</sup> BM cellularity. (G) CD45.1<sup>+</sup> Lin<sup>-</sup>/c-kit<sup>+</sup> BM cells. (H) CD45.1<sup>+</sup> LSK BM cells. Values shown are mean  $\pm$  SEM  $n \geq 5$  mice per group (\*\* $P < .01$ ).



### Engraftment of WT HSCs into OB/P Cx43-deficient HM is impaired through a homing defect.

HSC activity is characterized by their self-renewal ability in repopulation experiments where they rescue lethality after myeloablation. To evaluate the contribution of Cx43 in the HM to mediate HSC engraftment and repopulating efficiency, we analyzed the hematopoietic function of CD45.2<sup>+</sup> WT or OB/P Cx43-deficient mice transplanted with different doses of CD45.1<sup>+</sup> WT cells. A limiting cell dose as low as  $1 \times 10^4$  erythrocyte-lysed WT BM cells, rescued 50% of WT recipient mice, whereas all OB/P Cx43-deficient recipient mice died between day 8 and day 18 after transplantation ( $P < .01$ , Figure 1D). When the 2 groups of recipient mice were transplanted with a larger dose ( $3 \times 10^5$ ) of WT BM cells, both WT and OB/P Cx43-deficient recipients remained alive for more than 8 months with no differences in survival (data not shown); however, the long-term competitive repopulation was severely reduced in the OB/P-Cx43-deficient mice compared with the controls ( $P < .01$ ; Figure 1E). Chimerism levels of WT and OB/P Cx43-deficient recipient mice transplanted with a higher dose of WT BM cells ( $1 \times 10^6$ ), remained  $> 95\%$  for up to 14 months, and did not significantly differ between the WT and OB/P Cx43-deficient mice (data not shown).

To define the significance of Cx43-HM expression in long-term (LT)-HSC function, we transplanted BM from control or OB/P Cx43-deficient primary recipient mice (which had received  $1 \times 10^6$  BM CD45.1<sup>+</sup> cells in the primary transplant), into lethally irradiated secondary CD45.2<sup>+</sup> WT recipients. As previously mentioned,

in the primary recipients normal short-term (ST; 4 weeks) and LT (14 months) chimerism was seen in WT HSCs from either the WT or OB/P Cx43-deficient HM (data not shown). However, secondary recipient mice transplanted with WT HSCs that had previously resided in OB/P Cx43-deficient HM for 14 months showed increased mortality during the second month after transplantation ( $P < .05$ , Figure 2A). Death was because of pancytopenia in the presence of BM hypocellularity, loss of splenic follicle architecture, and severely diminished PB counts (Figure 2B-E, supplemental Figure 2A). Analysis of the BM compartment in the secondary recipient mice on day 71 after secondary transplantation (Figure 2A arrow), showed a reduction in total BM cellularity ( $188.9 \pm 10.1 \times 10^6$  BM cells in secondary recipients of WT BM engrafted in WT primary recipients versus  $48.6 \pm 13.8 \times 10^6$  BM cells in secondary recipients of WT BM engrafted in OB/P Cx43-deficient primary recipients;  $P < .01$ ), together with a dramatic reduction in the engraftment of CD45.1<sup>+</sup> BM donor cells, which had previously resided in the OB/P Cx43 deficient mice (Figure 2F). The reduced engraftment involved both myeloid and lymphoid populations (supplemental Figure 2B), and a dramatic reduction in the BM content of donor Lin<sup>-</sup>/c-kit<sup>+</sup> (Figure 2G) and LSK hematopoietic cells (Figure 2H). These data strongly indicated that the long-term WT hematopoietic graft in OB/P Cx43-deficient primary recipient mice was deprived of radioprotection and serial repopulation ability because of an extrinsic defect in the HM of OB/P Cx43-deficient mice.

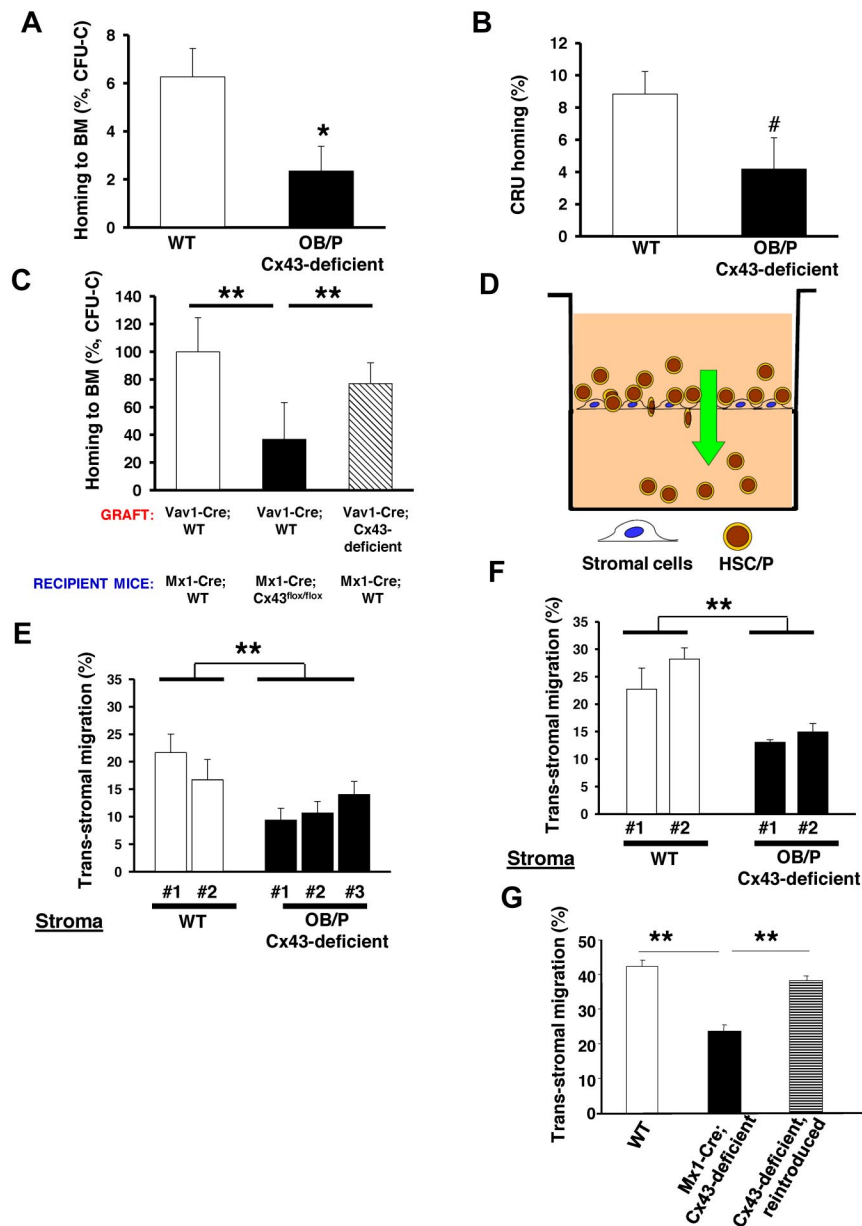


**Figure 3. BM homing of WT hematopoietic progenitor cells (HPCs) is impaired in myeloablated OB/P Cx43-deficient mice.** Impaired migration of HSC/Ps through irradiated Cx43-deficient stromal cell lines in a vitro assay. (A) Homing of BM CFU-C in the BM of either irradiated control (empty bar) or OB/P Cx43-deficient (solid bar) recipient mice at 16 hours after transplantation. A dramatic reduction in the ability of HPCs to home into the BM was seen when Cx43 is not expressed in the HM. (B) HSC homing assay in WT or OB/P Cx43-deficient mice. Graph represents homing (%) 3 hours after transplantation of CRUs as analyzed 20 weeks after transplantation into congenic recipients. The secondary recipients were injected with BM cells from primary WT or OB/P Cx43 deficient recipient mice that were previously transplanted with WT  $25 \times 10^6$  CD45.1<sup>+</sup> BM cells. Harvesting of BM cells from primary recipients was performed 3 hours after transplant. (C) Similarly to OB/P Cx43-deficient mice, homing of WT CFU-C to the BM of poly:I:C treated Mx1-Cre-Cx43<sup>flx/flx</sup> mice was drastically reduced compared with homing of either WT or Cx43-deficient HSC/P into Mx1-Cre;WT mice at 16 hours after transplantation. Data represent  $n = 4$  independent experiments with 5 mice per group and experiment. (D) Experimental scheme of the transstromal migration assay. LDBM cells were incubated on a monolayer of BM stromal cells previously layered on a transwell membrane. A Cxcl12 gradient was established from bottom to top of the transwell. (E-F) Transstromal migration of WT (E) or Cx43-deficient (F) HSC/Ps through WT or Cx43-deficient stromal cells. Migration of WT or Cx43-deficient HSC/Ps was similarly impaired when assayed in presence of WT or Cx43-deficient stromal cells. (G) Transstromal migration was restored on reintroduction of rat-Cx43 expression (gray bar) into Cx43-deficient stromal cell lines. Results from WT controls (empty bars) and mock-transduced, Mx1-Cre;Cx43-deficient stromal cells (solid bar) are also depicted. Data for homing experiments are shown as mean  $\pm$  SEM of 3 independent experiments, with a minimum of 7 mice per group. Data for transstromal migration are shown as mean  $\pm$  SEM  $n = 4$  independent experiments ( $*P < .05$ ;  $**P < .01$ ;  $***P < .001$ ;  $\#P = .08$ ).

To explore the mechanism associated with the engraftment defect, we performed a homing assay of WT BM cells into lethally irradiated OB/P-Cx43-deficient or control recipient mice. Under these experimental conditions, there was an approximate 60% reduction in the ability of the WT hematopoietic progenitors to home into irradiated Cx43-deficient BM compared with control mice (Figure 3A). Similar to what was shown in other models of defective homing of HSCs,<sup>30</sup> this homing defect did not translate into an increase of the fraction of circulating WT HSC/Ps in OB/P Cx43-deficient mice, as assessed by their immunophenotype Lin<sup>-</sup>/c-kit<sup>+</sup>/Sca-1<sup>+</sup> (LSK) and Lin<sup>-</sup>/c-kit<sup>+</sup>/Sca-1<sup>-</sup> (LK<sup>+</sup>S<sup>-</sup>) at 16 hours after transplantation (supplemental Figure 2C). The deficiency of Cx43 in the HM not only compromises the homing efficiency of hematopoietic progenitors but also the HSC population, because the long-term CRU populations showed reduced homing in OB/P Cx43-deficient mice (Figure 3B). We then tested whether the homing defect could be attributable exclusively to a Cx43-deficiency in the OB/P compartment from birth (OB/P mice model) or a Cx43 deficient HM induced during adulthood (Mx1-

Cre mice model). In Mx1-Cre;Cx43<sup>flx/flx</sup> macrophage-depleted BM stromal cells Cx43 expression was practically abrogated (supplemental Figure 3C). The homing of WT hematopoietic progenitors was similarly impaired in Mx1-Cre mice where the BM HM was Cx43-deficient (Figure 3C). Curiously we did not find a homing defect when Cx43 was specifically absent from hematopoietic progenitors (from Vav1-Cre-mice, compare dashed bar with empty bars, Figure 3C), indicating the exclusive dependence of Cx43 in the HM mediating the homing process in myeloablated animals. Altogether, these data indicate that the BM homing of HSC/P is severely reduced in Cx43-deficient irradiated HM.

#### HM Cx43 deficiency impairs the migration of hematopoietic progenitors through irradiated stroma

We analyzed the cellular mechanism of the homing defect, which was induced by the deficiency of Cx43 in the HM. We hypothesized that an OB/P Cx43 deficiency may result in defects in the HSC/P migration through the Cx43-deficient HM, similar to what

has been shown in neural migration along radial glia during development.<sup>18,19</sup> We studied the capacity of Cx43-deficient stromal cells to support the migration of HSC/Ps in vitro (Figure 3D). In this novel assay, similar to transendothelial migration assays, we analyzed the ability of HSC/Ps to migrate through irradiated stromal cells toward a gradient of Cxcl12. This assay is intended to model the physiologic migration of HSC/Ps through a subendothelial layer of irradiated stromal cells. There was a reduction of approximately 50% in the migration of WT hematopoietic progenitors through BM Cx43-deficient, macrophage-depleted stromal cell propagated explants (Figure 3E). The transstromal migration of Cx43-deficient HSC/Ps (Figure 3F) was reduced and was similar to the migration of WT progenitors through Cx43-deficient stromal cell lines (compare Figures 3E-F). This reduction in the migration of WT HSC/Ps through the OB/P Cx43-deficient BM stroma was not associated with a reduction in firm adhesion (supplemental Figure 2D), suggesting that firm adhesion of HSC/Ps is not mechanically responsible for the defective transstromal migration of HSC/Ps through OB/P Cx43-deficient stroma.

To discern whether Cx43 expression specifically controls the transstromal migration of HSC/Ps, we expressed rat Cx43 cDNA in Cx43-deleted macrophage-depleted stromal cells, which were obtained from OB/P Cx43-deficient mice (induced during fetal development). Although the transduction of rat Cx43 cDNA into Cx43-deficient cells derived from OB/P Cx43-deficient mice (supplemental Figure 3A) restored cell-to-cell dye transfer (data not shown), it did not restore their transstromal migration ability (supplemental Figure 3B). In contrast to the ineffectiveness of Cx43 reintroduction to restore the migration of HSC/P through OB/P Cx43-deficient stromal cell lines, exogenous Cx43 expression in Mx1-Cre; Cx43-deficient stromal cells (supplemental Figure 3D) did restore both cell-to-cell calcein transfer (supplemental Figure 4A-D) and transstromal migration of WT HSC/Ps (Figure 3G dashed bar), suggesting that the deficient migration of WT HSC/Ps through Cx43-deficient stroma may be a result of an irreversible modification in the cell composition of the BM HM in vivo.

#### Cx43 expression in the OB/P HM controls HSC/P lodgment, retention and mobilization in nonmyeloablated animals

Cx43 expression has been shown to be up-regulated up to 80-fold in the BM of irradiated animals.<sup>17</sup> We hypothesized that Cx43 up-regulation during irradiation may represent a determinant of HSC homing and that could differ from the Cx43 contribution to the homing and/or retention of HSC/Ps in the OB/P niche in nonmyeloablated conditions. We performed a group of experiments directed to analyze the homing and retention of HSC/Ps in nonmyeloablated OB/P Cx43-deficient animals.

We first analyzed the content of circulating HSC/Ps in OB/P Cx43-deficient mice and, found that the number of circulating hematopoietic progenitors (assessed by a CFU-C assay) was diminished by ~30% in the OB/P Cx43-deficient mice compared with WT mice (Figure 4A). This finding was confirmed at the HSC level by transplantation of blood from WT or OB/P Cx43-deficient animals in a competitive repopulation assay, where WT mice transplanted with PB from OB/P Cx43 deficient mice showed an ~60% reduction in the content of circulating competitive repopulating cells compared with control mice (Figure 4B). There were no differences between WT and OB/P Cx43-deficient mice in the content of hematopoietic progenitors in the spleen (supplemental Figure 5A), suggesting that the reduction of circulating HSC/Ps may associate exclusively with the increased retention of HSC/Ps

in the BM osteogenic HM. Furthermore, Cx43-deficient mice treated with granulocyte colony-stimulating factor (G-CSF) did not mobilize as well as WT animals (Figure 4C) and show higher HSC/P numbers in BM after G-CSF administration (Figure 4D). Correlating with the higher retention of HSC/Ps within a HM-Cx43-deficient, nonirradiated recipient OB/P Cx43-deficient mice receiving BM from Cx43 WT, ubiquitin C-EGFP transgenic congenic animals showed fewer circulating HSC/P (LSK and LK<sup>+</sup>S<sup>-</sup>) cells in the PB compared with WT counterparts at 16 hours after transplantation (Figure 4E). Although the organ homing of WT HSC/Ps in OB/P Cx43-deficient mice was unaltered (supplemental Figure 5B), the lodgment of fluorescently labeled WT hematopoietic progenitors into nonmyeloablated recipients, followed by in vivo multiphoton microscopy<sup>24,29</sup> showed that the distance between the transplanted HSC/Ps and the endosteum was significantly smaller in OB/P Cx43-deficient tibiae ( $23.2 \pm 0.9 \mu\text{m}$  vs  $34.3 \pm 6.8 \mu\text{m}$ , respectively;  $P < .01$ ; Figure 4F-G). In contrast to the deficient migration of HSC/Ps through irradiated Cx43-deficient stroma, the migration of HSC/Ps through Cx43-deficient, nonirradiated stroma was permissive for HSC/P migration (supplemental Figure 5C). These results indicate that Cx43 gene deletion in the nonmyeloablated BM OB/P compartment perturbs the endosteal lodgment, retention, and mobilization of HSC/Ps, and suggest the existence of an alternative mechanism of HSC/P lodgment and retention dependent on OB/P Cx43 expression.

#### OB/P Cx43 deficiency results in in vivo expansion of Cxcl12-expressing BM cells and increased level of Cxcl12 in the BM of nonmyeloablated mice

The retention of HSC/Ps relates to their ability to respond to chemoattractant gradients, which induce HSC/P retention in specific regions within the BM HM. OB/Ps express and secrete the BM chemoattractant Cxcl12, which is a crucial molecule mediating the retention and homing of HSC/Ps.<sup>31-33</sup> The binding of Cxcl12 to its receptor Cxcr4 provides signals that regulate the adhesion and interaction of HSC/Ps within specific niches in the subendosteal region (reviewed in Levesque et al<sup>34</sup>).

To analyze whether a change in the level of Cxcl12 is related to the higher retention of HSC/Ps in the BM of OB/P Cx43-deficient animals, we first analyzed the BM levels of Cxcl12 in vivo. We observed that both overall expression (Figure 5A) and extracellular Cxcl12 levels (Figure 5B) were both significantly increased in the BM of nonmyeloablated, OB/P Cx43-deficient mice, when compared with BM from control mice. These results were confirmed in 3 different stromal cell lines derived from OB/P Cx43-deficient mice. There was an almost 10-fold increase in the expression and secretion of Cxcl12 in these stromal cells compared with stromal cell lines derived from WT animals (supplemental Figure 5D-E). Interestingly, while BM myeloablation increased the BM extracellular level of Cxcl12 in WT mice, it failed to do so in OB/P Cx43-deficient mice (Figure 5B). The increased expression and secretion of Cxcl12 of nonmyeloablated OB/P Cx43 deficient animals was maintained after administration of G-CSF (Figure 5C-D), a HSC mobilizer, which is able to significantly decrease the level of BM Cxcl12.<sup>33</sup>

OB/P Cx43-deficient animals show osteogenic defects from birth.<sup>20</sup> We hypothesized that OB/P Cx43 deficiency results in a modified cellular composition of the BM mesenchymal cell populations in vivo that could be related to the observed increase in Cxcl12 levels. Therefore, we analyzed the content of mesenchymal progenitors (CFU-Fs), osteoblastic progenitors (CFU-OBs) and other osteogenic-lineage cells in the BM of OB/P Cx43-deficient

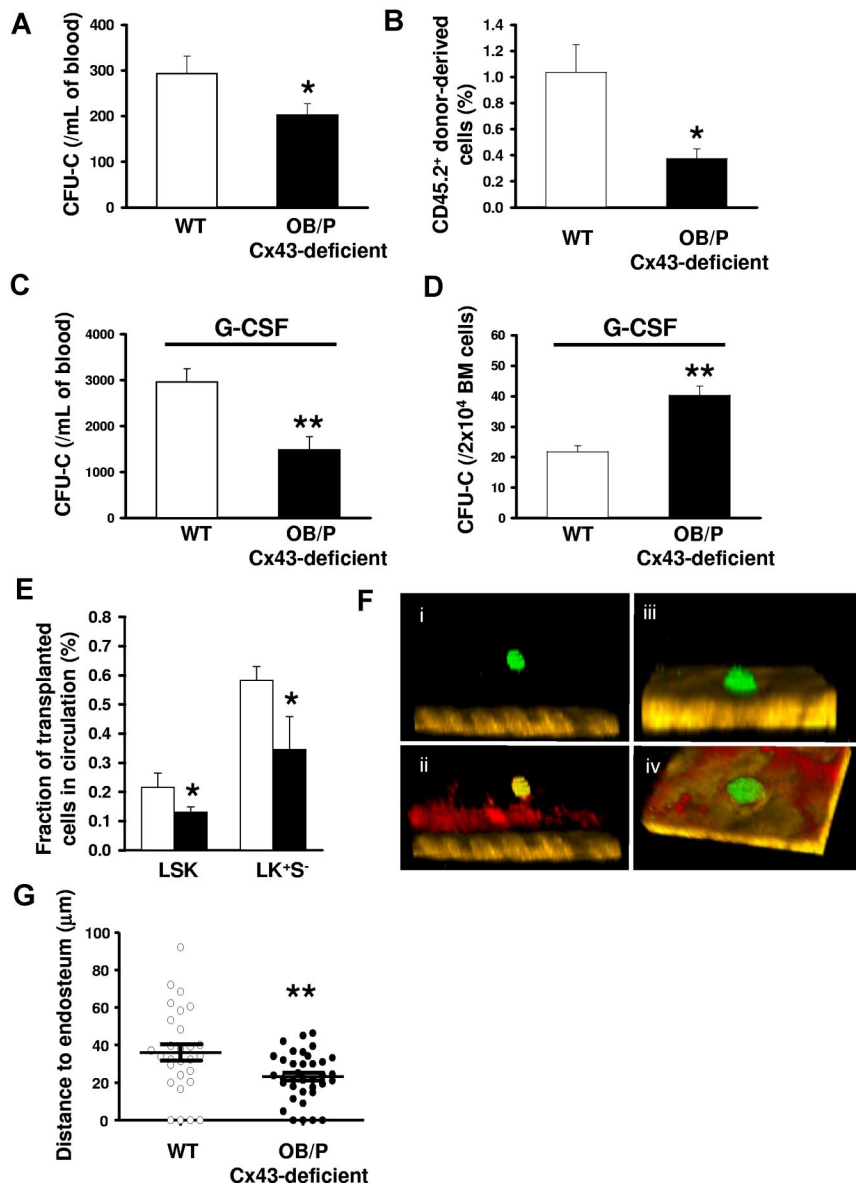


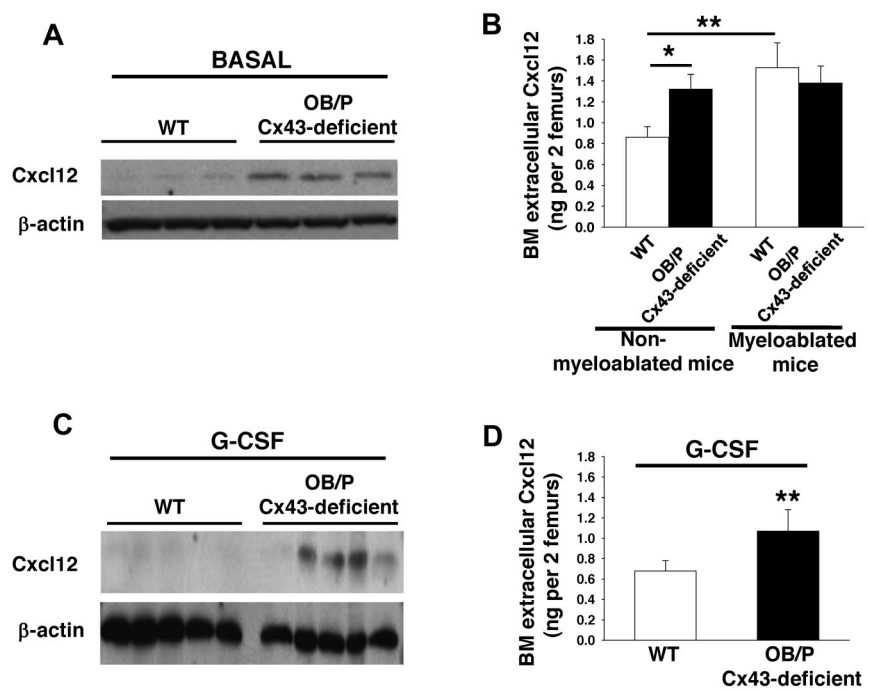
**Figure 4.** HSC/Ps are retained basally or after G-CSF administration, and located closer to the endosteum in the BM of nonmyeloablated OB/P Cx43-deficient mice. (A) PB CFU-C counts in WT (empty bar) and OB/P Cx43-deficient mice (solid bar). N = 4 independent experiments, n = 5 mice per group. (B) Percentage of chimerism in WT CD45.1<sup>+</sup> lethally irradiated recipient mice, which were transplanted with a mixture of  $5 \times 10^5$  WT CD45.2<sup>+</sup> WT or OB/P Cx43-deficient donors. N = 2 independent experiments, n = 5 mice per group. (C) Count of circulating HSC/Ps after G-CSF administration in WT and OB/P Cx43-deficient mice. N = 3 independent experiments, n = 5 mice per group. (D) Hematopoietic progenitor content of BM of G-CSF treated WT and OB/P Cx43-deficient mice. N = 3 independent experiments, n = 5 mice per group. (E) Nonirradiated WT or OB/P Cx43-deficient mice were transplanted with WT BM-EGFP<sup>+</sup> cells. Percentage of EGFP<sup>+</sup> LSK and LK<sup>+</sup>S<sup>-</sup> cell populations, determined by flow cytometry, in the PB 16 hours after transplantation. N = 2 independent experiments, n = 7-8 mice per group. Data are shown as mean  $\pm$  SEM. (F-G) In vivo imaging using multiphoton microscopy technique of transplanted CFSE-labeled hematopoietic progenitors (Lin<sup>-</sup>c-kit<sup>+</sup> BM cells average n > 25) clustered closer to the endosteum in OB/P Cx43-deficient mice than in controls (empty circles; n = 2 independent experiments). HSC/Ps were stained with CFSE directly after isolation and transplanted into WT or OB/P Cx43-deficient mice. After 24 hours intravital multiphoton imaging was performed in the tibiae of the recipient animals. (F) HSC/Ps (displayed in green) located distantly from the bone (brown, detected by its SHG signal) in the tibia of a WT recipient. (ii) In addition, the blood vessels could be detected after an intravenous injection of rhodamine-dextran (displayed in red). IVM was performed using a Zeiss LSM-710 microscope with simultaneous detection via external nondescanned detectors and Zeiss ZEN software (2009 release). Illumination was performed at 800 or 850 nm using a MaiTai TiSa laser via a 20 $\times$  water-dipping lens with 1.0 NA. Images were recorded every 60 seconds. Raw data were reconstructed using Volocity 4.0 software (PerkinElmer/Improvision). The dimensions of the original Z-stack were: X = 85.53  $\mu$ m; Y = 85.53  $\mu$ m; and Z = 108  $\mu$ m. The image resolution (XYZ) was 512  $\times$  512  $\times$  28  $\mu$ m. The pixel size was 0.167  $\mu$ m in X and Y and 4  $\mu$ m in Z. (iii) HSC/Ps (displayed in green) in close contact to the endosteum (brown, detected by its SHG signal) in the tibia of an OB/P Cx43-deficient mouse. (iv) After an injection of rhodamine-dextran also the blood vessels could be detected (displayed in red). The dimensions of the original Z-stack were: X = 227.36  $\mu$ m and Y = 227.36  $\mu$ m; Z = 92  $\mu$ m. Image resolution (XYZ) was 512  $\times$  512  $\times$  28  $\mu$ m. One pixel in X and Y are equivalent to 0.445  $\mu$ m and in Z = 4  $\mu$ m. (G) Distance to endosteum of individual HSC/P analyzed in vivo. Transversal bars denote mean  $\pm$  SEM (\*P < .05; \*\*P < .01).

mice. A 2- and 3-fold increase in the number of CFU-Fs (Figure 6A) and CFU-OBs (Figure 6B) was observed, indicating that Cx43 deficiency induces a significant expansion of the mesenchymal and osteoprogenitor compartment in the BM. The increase in nonhematopoietic cells in the BM was confirmed by a quantitative flow cytometry analysis of Cxcl12-expressing, CD45<sup>-</sup>/Ter119<sup>-</sup> BM cells in OB/P Cx43-deficient mice. Quantitative analysis of nonhematopoietic subpopulations revealed an approximately 2-fold increase in the content of nonosteogenic mesenchymal CD45<sup>-</sup>/Ter119<sup>-</sup>/cadherin-11<sup>-</sup> cells (Figure 6C-D), while the pool of OB/P cells (CD45<sup>-</sup>/Ter119<sup>-</sup>/cadherin-11<sup>+</sup>) in the BM was not significantly changed (Figure 6E). The frequency of Cxcl12-expressing cells in OB/P Cx43-deficient BM was increased in the CD45<sup>-</sup>/Ter119<sup>-</sup>/cadherin-11<sup>+</sup> cell fraction and, even more, in the CD45<sup>-</sup>/Ter119<sup>-</sup>/cadherin-11<sup>-</sup> cell popu-

lation (~ 2- and 3.5-fold, respectively; Figure 6F-G) indicating that OB/P Cx43-deficient mice contained a larger fraction of Cxcl12-expressing HM cells in both the osteogenic and nonosteogenic fractions. This expansion of Cxcl12-expressing mesenchymal cells was due to increased proliferation in vivo (Figure 6H-I) and was associated with ~ 90% decreased levels of sclerostin (Sost) expression (Figure 6J), an osteocyte-expressed hormonal negative regulator on MSC and osteoprogenitor proliferation.<sup>35</sup>

Altogether, our data indicate that OB/P Cx43 is indispensable to allow HSC homing in irradiated recipients and acts as a regulator of HSC traffic in and of the stem cell niche, directly through impaired migration through irradiated HM, and indirectly through control of the BM Cxcl12-expressing cell composition. The deficiency of Cx43 in OB/P induces quantitative and functional changes in the

**Figure 5. Cxcl12 expression and secretion are increased in OB/P Cx43-deficient BM.** (A-C) Western blot of whole BM lysates analyzed for Cxcl12 expression basally (A) and after G-CSF administration (C). (B-D) Extracellular BM Cxcl12 levels determined by ELISA in WT and OB/P Cx43-deficient BM from steady-state and lethally irradiated mice (16 hours after irradiation; B) and in nonmyeloablated mice after G-CSF administration (D). Empty bars represent control (WT) values and solid bars represent OB/P Cx43-deficient values. Data are shown as mean  $\pm$  SEM of 3 independent experiments with a minimum of 5 mice per group (\* $P$  < .05; \*\* $P$  < .01).



HM related to its ability to allow bidirectional trafficking (homing and mobilization) of HSC/Ps and increased content of Cxcl12-expressing mesenchymal cells.

## Discussion

The specific cellular microenvironment in which HSCs reside within the BM cavity, termed a “niche” is required for correct HSC function under basal and stress conditions. A complex interplay of cytokines, chemokines, proteolytic enzymes, and adhesion molecules maintain HSC-anchorage to the niche infrastructure. A generic group of mesenchymal-lineage stromal cells, encompassing osteoblasts,<sup>4,6</sup> N-cadherin<sup>+</sup> preosteoblastic cells,<sup>36</sup> CXCL12 abundant reticular (CAR) cells,<sup>3</sup> osteoblastic progenitors,<sup>37</sup> and so-called MSCs,<sup>5</sup> have been shown to play a signaling role in the control of the composition and function of HSC niches.

In HSC transplantation, for a successful engraftment, the transplanted HSCs must first home to the BM, and then localize and anchor in suitable microenvironments within the BM, a process known as lodgment.<sup>12</sup> Although the fate of nonlodged HSC/Ps is unclear, a fraction of BM HSC/Ps may not survive, and another cell fraction may circulate in the PB in a highly regulated process of HSC traffic.

Our understanding of the HM in relation to HSC traffic has significantly advanced. The HM is connected through the sympathetic nervous system,<sup>38</sup> which controls the expression and release of Cxcl12 through the stimulation of  $\beta_3$ -adrenergic receptors in stromal cells,<sup>5</sup> and therefore modulates the migration of HSC/Ps. Postganglionic sympathetic fibers in the BM are associated with blood vessels, and adventitial reticular cells connected by GJ, together form a pseudosynchytial structural network. GJ-like structures in the BM were identified 30 years ago,<sup>39</sup> and the first functional relationship between GJ structures and the HM was seen in the increased numbers of GJ structures in the stromal cells of stromal-dependent stem cell factor-deficient (Sl/Sl<sup>d</sup>) mice.<sup>40</sup>

Cx43 has been shown to be the predominant Cx in BM stromal cells and in osteoblasts,<sup>41</sup> and is also expressed by HSCs.<sup>10</sup> A latent network of Cx43-dependent GJIC in normal quiescent marrow has been proposed, which may be up-regulated in neonatal marrow or after forced stem cell division.<sup>17</sup> Outside of the BM, the deficiency of Cx43 has been shown to induce increased cell proliferation in vitro and in vivo, through the loss of its tumor suppressor functions,<sup>42,43</sup> and to regulate the migration of neural progenitors in contact with radial glia during brain development.<sup>18,19</sup>

Using a murine model, in which Cx43 deficiency was specifically induced in osteoblasts and osteoprogenitors, we studied the function of Cx43 in the process of HSC/P migration in steady-state conditions and after transplantation in myeloablative and nonmyeloablative conditions. We found that the deletion of Cx43 in HM produces several, distinct short- and long-term effects on HSC/P migration and hematopoietic function, which are probably related to different functions exerted by Cx43 in the BM.

The function attributed to Cx43 as a regulator of cell migration in other non-BM tissues, led us to analyze whether Cx43 could mediate the migration of HSC/Ps. We analyzed the homing of HSC/Ps in myeloablative conditions, which significantly up-regulate the expression of Cx43<sup>17</sup> and Cxcl12<sup>16</sup> expression in the BM HM. Homing of progenitors and repopulating stem cells was defective in myeloablated OB/P Cx43-deficient mice as assessed by defective homing assays for both functional hematopoietic progenitors and competitive repopulating cells. The defective homing in myeloablated animals is biologically relevant because it results in both radioprotection failure and in long-term HSC engraftment failure of WT HSCs transplanted into OB/P Cx43-deficient recipients. The homing defect correlates with defective in vitro transstromal migration. The mechanism responsible for the migration defect does not require the expression of Cx43 by HSC/Ps, indicating that the Cx43-dependent heterocellular interaction between HSC/Ps and stromal cells is not implicated in this process. These results agree with our previous findings, which



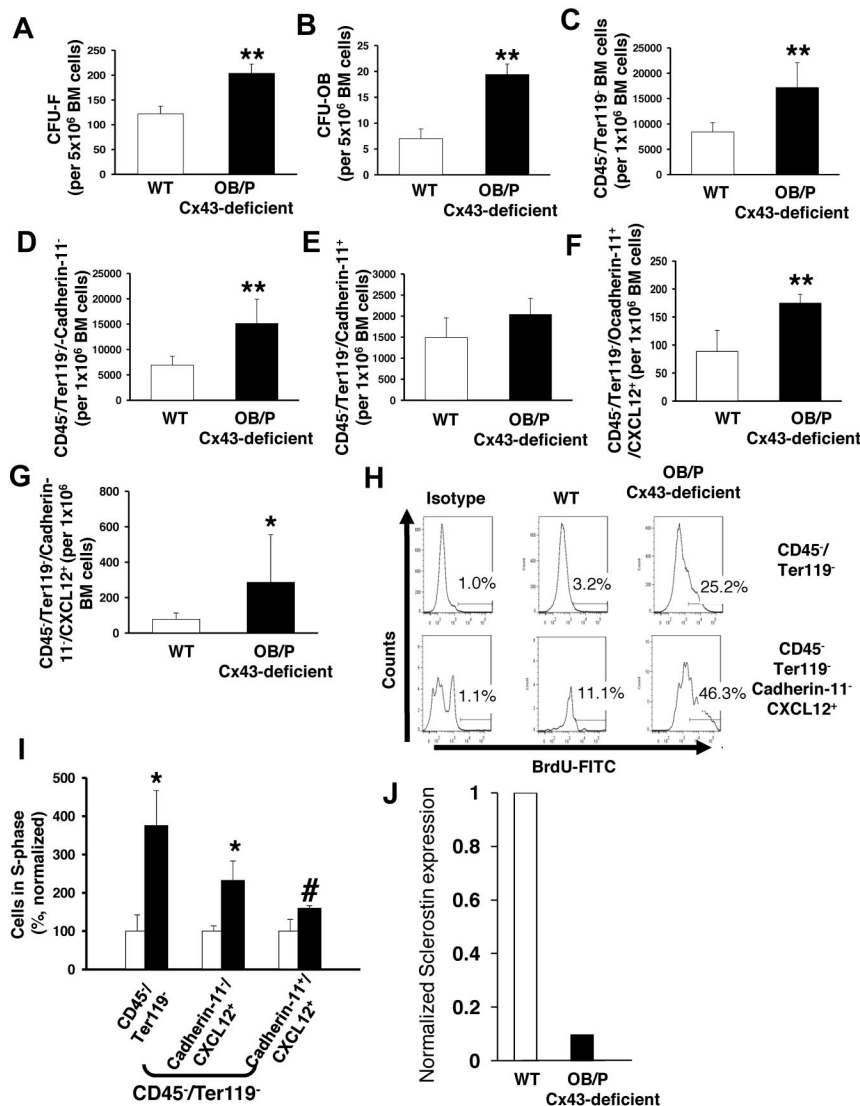


**Figure 6. Cx43 regulates the cellular composition in nonmyeloablated BM.** (A–B) Content of BM mesenchymal (CFU-F; A) and osteoblastic progenitors (CFU-OB; B) in BM of WT and OB/P Cx43-deficient mice. (C–E) Quantification of immunophenotypically identified nonhematopoietic cells (C) and cadherin-11 negative (D) or positive (E) subpopulations. (F–G) OB/P-Cx43-deficient mice showed an increased number of Cxcl12<sup>+</sup> cells among both CD45<sup>+</sup>/Ter119<sup>-</sup>/cadherin-11<sup>+</sup> and CD45<sup>+</sup>/Ter119<sup>-</sup>/cadherin-11<sup>-</sup> cell subpopulations. (H) Representative example of flow cytometry analysis of 5-bromo-2'-deoxyuridine (BrdU<sup>+</sup>) cells on different mesenchymal cell subpopulations. (I) In vivo proliferation of BM CD45<sup>+</sup>/Ter119<sup>-</sup> and Cxcl12<sup>+</sup> mesenchymal cells. (J) Normalized RNA expression of sclerostin in cortical bones from WT or OB/P Cx43-deficient mice. Results for sclerostin expression are presented as average of 2 mice per group where expression was analyzed in femora, tibiae, and pelvic cortical bones. Empty bars present control data; solid bars represent data from OB/P Cx43-deficient mice. Analysis of OB/P populations are shown as mean ± SD. N = 3 different experiments n = 6 mice per group (\*P < .05; \*\*P < .01).

showed that Cx43-deficiency of irradiated stroma impaired formation of CAFC,<sup>8</sup> a surrogate assay for HSC/P function, which depends on transstromal migration and provides in vivo and cellular mechanistic analysis of the defects associated with the hematopoiesis of Cx43-deficient BM. Rescue of both metabolic coupling, a crucial function of Cx43 in GJIC, and transstromal migration of HSC/Ps, through reexpression of Cx43 in inducible Cx43-deficient BM stromal cells, indicated that it is possible to restore the function of mesenchymal cells from inducible, short-term Cx43-deficient BM, but not from long-term OB/P Cx43-deficient BM. We hypothesized that the OB/P Cx43-deficient BM cell composition may be responsible for the lack of restoration of transstromal migration after Cx43 reintroduction.

In addition, we found that the cell composition of an OB/P Cx43-deficient microenvironment was significantly modified compared to that of WT mice. These mice showed an overall expansion of mesenchymal cells, including Cxcl12-expressing cells, which translates into increased levels of expression and secretion of Cxcl12 within the BM basally and after G-CSF administration. The expansion of mesenchymal/osteogenic progenitors with an increased ability to express and secrete Cxcl12 may be the result of

the decreased expression and/or secretion of one or several short-range acting factors, which have inhibitory activity on the proliferation of bone-forming progenitor cells. Among them, the expression level of sclerostin,<sup>44</sup> an osteocyte-expressed hormonal negative regulator of MSCs and osteoprogenitor proliferation<sup>35</sup> was found to be down-regulated in OB/P Cx43-deficient mice, which correlates with the increased BM content of osteoprogenitors.

BM Cxcl12 controls the migration of HSC/Ps between the BM and circulation,<sup>33</sup> and mesenchymal-lineage cells, including mesenchymal progenitors and osteolineage cells, act as cell effectors of Cxcl12 secretion.<sup>5,31</sup> The increased level of Cxcl12 expression and secretion induced by the long-term deficiency of osteolineage Cx43 in nonmyeloablated BM overrides the homing and impaired transstromal migration found in myeloablated mice or stroma, suggesting that OB/P Cx43 functions as a homing factor only in irradiated animals. Accordingly, we found a decreased number of circulating HSC/Ps (assessed by both progenitor and competitive repopulating assays) in nonmyeloablated OB/P Cx43-deficient mice in parallel with a reduced level of circulating HSC/Ps, suggesting a higher retention of HSC/Ps in the BM. Such a phenotype correlated with a significantly closer location of HSC/Ps to the endosteum of OB/P

Cx43-deficient bones, but not with increased BM homing or transstromal migration, suggesting the existence of an extrinsic mechanism that controls the microanatomical location of HSC/Ps in OB/P Cx43-deficient mice. Both the decreased circulation of HSC/Ps and the closer location of HSC/Ps to the bone endosteum corresponded to normal HSC/P transstromal migration and increased Cxcl12 expression and secretion by the HM of nonmyeloablated OB/P Cx43-deficient mice. Increased Cxcl12 expression levels may be due to the increased content of Cxcl12-expressing mesenchymal cells and osteoprogenitors in the BM. Recently it has been demonstrated that Cxcl12 secretion is diminished in BM stromal cells when GJIC is impaired by the nonspecific drug carbenoxolone.<sup>45</sup> A reduction in Cxcl12 secretion was also observed in vitro by using specific shRNA against Cx43 in stromal cells with previous Cx45 deficiency in their genetic background.<sup>45</sup> In contrast, it has been demonstrated that intercellular GJ channels in the BM stroma permit the transfer of small noncoding RNA, such as miR-197, an microRNA, which interferes with Cxcl12 expression, a phenomenon that can be relevant in physiologic and pathologic conditions.<sup>46</sup> Our model of OB/P Cx43 deficiency indicates that Cxcl12 secretion is highly dependent on the cellular context. After myeloablation in vitro or in vivo, the levels of Cxcl12 in WT BM increase as previously reported,<sup>16</sup> whereas the levels in OB/P Cx43-deficient BM remain at the same as in nonmyeloablated BM. The mechanism behind the lack of overproduction of Cxcl12 by OB/P Cx43-deficient BM after myeloablation is unclear; however, it may have to do with the intrinsic role of Cx43 on Cxcl12 secretion.<sup>45</sup> Our experiments clearly indicate that the deficiency of Cxcl12 secretion induced by Cx43 deficiency is observed after myeloablation but not in steady-state conditions.

This data establishes the role of Cx43 as a positive regulator of homing and engraftment in myeloablated recipients, reinforces the role of Cxcl12-expressing osteoprogenitors and mesenchymal cells as major constituents of the BM stem cell niche, and presents Cx43 as an indirect negative regulator of endosteal homing in nonmyeloablated animals. A defective “soil” induced by Cx43-deficiency

could be responsible for the bidirectional trafficking defect of HSCs in Cx43-deficient BM.

## Acknowledgments

The authors thank Dr David Williams (Boston Children’s Hospital, Harvard Medical School), Dr Yi Zheng (Cincinnati Children’s Hospital), and Dr Hartmut Geiger (University of Ulm) for their comments to improve the paper; and Ms Margaret O’Leary for editing the paper.

This study was supported by the Heimlich Institute of Cincinnati (J.A.C.), the Department of Defense (grant no. 10580355, J.A.C.), the National Institutes of Health (NIH; R01-HL087159 and HL087159S1, J.A.C.), the University of Cincinnati Fellowship Award (J.A.C.), the National Blood Foundation (D.G.-N.), the Spanish Ministry of Science and Technology (Consolider CSD2008-00005, L.C.B.), the Community of Madrid (S2010/BMD-2460, D.G.-N.), NIH R01 AR041255 (R.C.), and the Hoxworth Blood Center and Cincinnati Children’s Hospital Medical Center (J.A.C.).

## Authorship

Contribution: D.G.-N., L.L., A.K., G.G., E.I., A.S., M.M., J.L.A., R.A.S., S.K.D., and J.A.C. performed experiments; D.G.-N., A.K., and J.A.C. analyzed data and interpreted results; D.E.G., G.I.F., and R.C. provided crucial reagents; and D.G.-N., R.C., L.C.B., M.G., and J.A.C. wrote the paper.

Conflict-of-interest disclosure: The authors declare no competing financial interests.

Correspondence: Jose A. Cancelas, Division of Experimental Hematology & Cancer Biology, 3333 Burnet Ave, Cincinnati, OH 45267; or Hoxworth Blood Center, University of Cincinnati, 3130 Highland Ave, Cincinnati, OH 45267-0055; e-mail: jose.cancelas@uc.edu.

## References

- Calvi LM, Adams GB, Weibrecht KW, et al. Osteoblastic cells regulate the haematopoietic stem cell niche. *Nature*. 2003;425(6960):841-846.
- Kiel MJ, Yilmaz OH, Iwashita T, Yilmaz OH, Terhorst C, Morrison SJ. SLAM family receptors distinguish hematopoietic stem and progenitor cells and reveal endothelial niches for stem cells. *Cell*. 2005;121(7):1109-1121.
- Sugiyama T, Kohara H, Noda M, Nagasawa T. Maintenance of the hematopoietic stem cell pool by CXCL12-CXCR4 chemokine signaling in bone marrow stromal cell niches. *Immunity*. 2006; 25(6):977-988.
- Zhang J, Niu C, Ye L, et al. Identification of the hematopoietic stem cell niche and control of the niche size. *Nature*. 2003;425(6960):836-841.
- Mendez-Ferrer S, Michurina TV, Ferraro F, et al. Mesenchymal and hematopoietic stem cells form a unique bone marrow niche. *Nature*. 2010; 466(7308):829-834.
- Lo Celso C, Fleming HE, Wu JW, et al. Live-animal tracking of individual hematopoietic stem/progenitor cells in their niche. *Nature*. 2009; 457(7225):92-96.
- Harris AL. Connexin channel permeability to cytoplasmic molecules. *Prog Biophys Mol Biol*. 2007; 94(1-2):120-143.
- Cancelas JA, Koevoet WL, de Koning AE, Mayen AE, Rombouts EJ, Ploemacher RE. Connexin-43 gap junctions are involved in multicellular DNA damage improves human stem cell function. *J Clin Invest*. 2000;106(11):1331-1339.
- Rosendaal M, Green CR, Rahman A, Morgan D. Up-regulation of the connexin43+ gap junction network in haematopoietic tissue before the growth of stem cells. *J Cell Sci*. 1994;107(Pt 1):29-37.
- Elias LA, Wang DD, Kriegstein AR. Gap junction adhesion is necessary for radial migration in the neocortex. *Nature*. 2007;448(7156):901-907.
- Cina C, Maass K, Theis M, Willecke K, Bechberger JF, Naus CC. Involvement of the cytoplasmic C-terminal domain of connexin43 in neuronal migration. *J Neurosci*. 2009;29(7):2009-2021.
- Chung DJ, Castro CH, Watkins M, et al. Low peak bone mass and attenuated anabolic response to parathyroid hormone in mice with an osteoblast-specific deletion of connexin43. *J Cell Sci*. 2006;119(Pt 20):4187-4198.
- Hens JR, Wilson KM, Dann P, Chen X, Horowitz MC, Wysolmerski JJ. TOPGAL mice show that the canonical Wnt signaling pathway is active during bone development and growth and is activated by mechanical loading in vitro. *J Bone Miner Res*. 2005;20(7):1103-1113.
- Sengupta A, Duran A, Ishikawa E, et al. Atypical protein kinase C (aPKC[ $\zeta$ ] and aPKC[ $\lambda$ ]) is dispensable for mammalian hematopoietic stem cell activity and blood formation. *Proc Natl Acad Sci U S A*. 2011;108(24):9957-9962.
- Schaefer BC, Schaefer ML, Kappler JW, expressing stromal support of hemopoietic progenitors and stem cells. *Blood*. 2000;96(2):498-505.
- Civitelli R. Cell-cell communication in the osteoblast/osteocyte lineage. *Arch Biochem Biophys*. 2008;473(2):188-192.
- Forsberg EC, Prohaska SS, Katzman S, Heffner GC, Stuart JM, Weissman IL. Differential expression of novel potential regulators in hematopoietic stem cells. *PLoS Genet*. 2005;1(3):e28.
- Durig J, Rosenthal C, Halfmeyer K, et al. Intercellular communication between bone marrow stromal cells and CD34+ hematopoietic progenitor cells is mediated by connexin 43-type gap junctions. *Br J Haematol*. 2000;111(2):416-425.
- Lam BS, Adams GB. Hemopoietic stem cell lodgment in the adult bone marrow stem cell niche. *Int J Lab Hematol*. 2010;32(6 Pt 2):551-558.
- Bexell D, Gunnarsson S, Tormin A, et al. Bone marrow multipotent mesenchymal stroma cells act as pericyte-like migratory vehicles in experimental gliomas. *Mol Ther*. 2009;17(1):183-190.
- Czechowicz A, Kraft D, Weissman IL, Bhattacharya D. Efficient transplantation via antibody-based clearance of hematopoietic stem cell niches. *Science*. 2007;318(5854):1296-1299.
- Greenberger JS. Toxic effects on the hematopoietic microenvironment. *Exp Hematol*. 1991; 19(11):1101-1109.
- Ponamaryov T, Peled A, Petit I, et al. Induction of the chemokine stromal-derived factor-1 following

- Marrack P, Kiedl RM. Observation of antigen-dependent CD8+ T-cell/dendritic cell interactions in vivo. *Cell Immunol*. 2001;214(2):110-122.
24. Ryan MA, Nattamai KJ, Xing E, et al. Pharmacological inhibition of EGFR signaling enhances G-CSF-induced hematopoietic stem cell mobilization. *Nat Med*. 2010;16(10):1141-1146.
25. Cheng SL, Lecanda F, Davidson MK, et al. Human osteoblasts express a repertoire of cadherins, which are critical for BMP-2-induced osteogenic differentiation. *J Bone Miner Res*. 1998;13(4):633-644.
26. Cancelas JA. Adhesion, migration, and homing of murine hematopoietic stem cells and progenitors. *Methods Mol Biol*. 2011;750:187-196.
27. Cancelas JA, Lee AW, Prabhakar R, Stringer KF, Zheng Y, Williams DA. Rac GTPases differentially integrate signals regulating hematopoietic stem cell localization. *Nat Med*. 2005;11(8):886-891.
28. Boggs DR. The total marrow mass of the mouse: a simplified method of measurement. *Am J Hematol*. 1984;16(3):277-286.
29. Kohler A, Schmithorst V, Filippi MD, et al. Altered cellular dynamics and endosteal location of aged early hematopoietic progenitor cells revealed by time-lapse intravital imaging in long bones. *Blood*. 2009;114(2):290-298.
30. Foudi A, Jarrier P, Zhang Y, et al. Reduced retention of radioprotective hematopoietic cells within the bone marrow microenvironment in CXCR4<sup>-/-</sup> chimeric mice. *Blood*. 2006;107(6):2243-2251.
31. Christopher MJ, Liu F, Hilton MJ, Long F, Link DC. Suppression of CXCL12 production by bone marrow osteoblasts is a common and critical pathway for cytokine-induced mobilization. *Blood*. 2009;114(7):1331-1339.
32. Peled A, Grabovsky V, Habler L, et al. The chemokine SDF-1 stimulates integrin-mediated arrest of CD34(+) cells on vascular endothelium under shear flow. *J Clin Invest*. 1999;104(9):1199-1211.
33. Petit I, Szyper-Kravitz M, Nagler A, et al. G-CSF induces stem cell mobilization by decreasing bone marrow SDF-1 and up-regulating CXCR4. *Nat Immunol*. 2002;3(7):687-694.
34. Levesque JP, Helwani FM, Winkler IG. The endosteal 'osteoblastic' niche and its role in hematopoietic stem cell homing and mobilization. *Leukemia*. 2010;24(12):1979-1992.
35. Li X, Ominsky MS, Niu QT, et al. Targeted deletion of the sclerostin gene in mice results in increased bone formation and bone strength. *J Bone Miner Res*. 2008;23(6):860-869.
36. Xie Y, Yin T, Wiegraebe W, et al. Detection of functional haematopoietic stem cell niche using real-time imaging. *Nature*. 2009;457(7225):97-101.
37. Raaijmakers MH, Mukherjee S, Guo S, et al. Bone progenitor dysfunction induces myelodysplasia and secondary leukaemia. *Nature*. 2010;464(7290):852-857.
38. Katayama Y, Battista M, Kao WM, et al. Signals from the sympathetic nervous system regulate hematopoietic stem cell egress from bone marrow. *Cell*. 2006;124(2):407-421.
39. Campbell FR. Gap junctions between cells of bone marrow: an ultrastructural study using tannic acid. *Anat Rec*. 1980;196(1):101-107.
40. Yamazaki K. Sl/Slid mice have an increased number of gap junctions in their bone marrow stromal cells. *Blood Cells*. 1988;13(3):421-435.
41. Dorshkind K, Green L, Godwin A, Fletcher WH. Connexin-43-type gap junctions mediate communication between bone marrow stromal cells. *Blood*. 1993;82(1):38-45.
42. Francis RJ, Lo CW. Primordial germ cell deficiency in the connexin 43 knockout mouse arises from apoptosis associated with abnormal p53 activation. *Development*. 2006;133(17):3451-3460.
43. Sridharan S, Simon L, Meling DD, et al. Proliferation of adult sertoli cells following conditional knockout of the Gap junctional protein GJA1 (connexin 43) in mice. *Biol Reprod*. 2007;76(5):804-812.
44. Watkins M, Grimston SK, Norris JY, et al. Osteoblast connexin43 modulates skeletal architecture by regulating both arms of bone remodeling. *Mol Biol Cell*. 2011;22(8):1240-1251.
45. Schajnovitz A, Itkin T, D'Uva G, et al. CXCL12 secretion by bone marrow stromal cells is dependent on cell contact and mediated by connexin-43 and connexin-45 gap junctions. *Nat Immunol*. 2011;12(5):391-398.
46. Lim PK, Bliss SA, Patel SA, et al. Gap junction-mediated import of microRNA from bone marrow stromal cells can elicit cell cycle quiescence in breast cancer cells. *Cancer Res*. 2011;71(5):1550-1560.